Coordinate-free formation control of multi-agent systems using rooted graphs

Liu, Hui; Lin, Zhiyun; Cao, Ming; Wang, Xiaoping; Lv, Jinhu

Published in:
Systems & Control Letters

DOI:
10.1016/j.sysconle.2018.06.006

Publication date:
2018

Coordinate-free Formation Control of Multi-agent Systems Using Rooted Graphs

Hui Liu[a,*], Zhiyun Lin[b,*], Ming Cao[c], Xiaoping Wang[a], Jinhu Lü[d]

[a] *School of Automation & Key Laboratory of Image Processing and Intelligent Control of Education Ministry of China, Huazhong University of Science and Technology, 430074 Wuhan, China.*

[b] *Hangzhou Dianzi University, Hangzhou 310018, China*

[c] *Engineering and Technology Institute, University of Groningen, 9747 AG Groningen, The Netherlands.*

[d] *Academy of Mathematics and Systems Science, Chinese Academy of Sciences, 100190 Beijing, China.*

Abstract

This paper studies how to control large formations of autonomous agents in the plane, assuming that each agent is able to sense relative positions of its neighboring agents with respect to its own local coordinate system. We tackle the problem by adopting two types of controllers. First, we use the classical gradient-based controllers on three leader agents to meet their distance constraints. Second, we develop other type of controllers for follower agents: utilizing the properties of rooted graphs, one is able to design linear controllers incorporating relative positions between the follower agents and their neighbors, to stabilize the overall large formations. The advantages of the proposed method are fourfold: *i)* fewer constraints on neighboring relationship graphs; *ii)* simplicity of linear controllers for follower agents; *iii)* global convergence of the overall formations; *iv)* implementation in local coordinate systems, in no need of a global coordinate system. Numerical simulations show the effectiveness of the proposed method.

Keywords: Multi-agent system; Formation control; Graph theory; Stabilization.

1. Introduction

Distributed coordination of teams of autonomous robots has received increasing attention from the control society in the last decade [1, 2, 3, 4], due to the rapid development of computation and communication techniques as well as powerful embedded systems. One typical coordination task is formation keeping, in which a team of mobile agents is required to move collaboratively

*Corresponding author.

Email addresses: hliu@hust.edu.cn (Hui Liu), linz@hdu.edu.cn (Zhiyun Lin)

so that the team manoeuvres as a whole with a prescribed formation shape [5, 6, 7, 8, 9, 10]. Formation control of mobile agents, finds various applications in engineering fields, such as sensor networks for data collections [11], unmanned aerial vehicles for military missions [12], and satellite formations for deep space exploration [13].

Various approaches have been proposed to achieve formation stabilization, which can be generally categorized into position-, displacement-, and gradient-based control. Gradient-based control is also as known as distance-based control in some literature. A recent survey [14] of multi-agent formation control discussed the distinctions of the three categories in detail. Position-based control requires that all the agents in a formation-task group are capable of sensing their own positions with respect to a global coordinate system [15, 16, 17]. Displacement-based control requires that each mobile agent is equipped with a compass such that all the agents share a common sense of direction [18, 19, 20, 21]. Gradient-based formation control, in comparison, only requires that each mobile agent knows relative positions of its neighbors in its own local coordinate [22, 23, 24, 25, 26, 27]. To achieve the desired shape by controlling the distances between agents, the interaction graph needs to be rigid or persistent [5, 8]. The convergence results of gradient-based formation control only hold locally; in other words, a prescribed formation can be restored only when the agents' shape is close enough to the prescribed one. Global stability analysis has been carried out merely for a class of triangular formations [27, 28, 29]. However, the method is difficult to be applied to large formations, since the control laws involving Euclidean distances result in nonlinearity and multiple equilibrium manifolds, which significantly complicates the analysis for formation stabilization. There are some other approaches describe a formation by using bearing measures [30, 31].

In this paper, we study formation-keeping tasks in the plane for multiple autonomous agents in their local coordinates. We cope with the challenge by making use of the benchmark case of triangular formations. Existing results [27, 28, 29] about triangular formations have proven that under gradient-based control, the convergence to the desired triangular formation is almost global except for initially collinearly positioned formations. We are able to treat the three agents in the original triangular formation as leaders and then construct large formations by adding more agents. Using the properties of rooted graphs, we design linear controllers incorporating relative positions between the newly-added agents and their neighbors, to stabilize enlarged formations. Compared with the position-based control and displacement-based control methods, our proposed method is coordinate-free, i.e., mobile agents neither need a global coordinate, nor need to share a common sense of direction. Although the controllers are designed differently for the leader agents and for the follower agents, each agent in formation only needs to acquire *relative positions* of its neighbors in its own coordinate system. Compared with the gradient-based control method [5, 8, 22, 23, 24, 25], the advantages of our proposed method are threefold: *i)* The convergence of the formation for the whole group of agents is almost *global* except for the case when the positions of the three leaders are initially

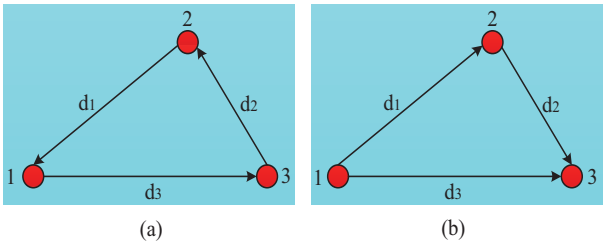

Figure 1: Prescribed formation shape. An edge from vertex i to j represents that j can measure the relative position of i. (a) Cyclic triangle. (b) Acyclic triangle.

collinear. *ii)* The controllers for the later added agents are linear, which are much simpler than the nonlinear gradient-based formation controllers. *iii)* our method requires fewer constraints on the neighbor-relationship graph $\mathbb{G}$, i.e., the graph is not required to be rigid.

The rest of the paper is organized as follows. In Section 2, we review a class of triangular formation models and the relevant results in the literature. Then in Section 3, using the properties of rooted graphs, we treat the three agents in the original triangular formation as leaders (i.e., roots) and propose a control method incorporating relative positions between the later added agents and their neighbors, to realize large formations. Furthermore, we prove global convergence for the formations with newly added agents in this section. Numerical examples are given in Section 4 to validate our theoretical analysis. Finally, we make concluding remarks in Section 5.

2. Review on Controlling Triangular Formations

In this section, we review some results in [26, 27, 28] about the benchmark case of triangular formations of autonomous agents.

We consider a formation in the plane consisting of three autonomous agents labeled by 1, 2, and 3, shown in Fig. 1. For $i \in \{1, 2, 3\}$, we use $[i]$ to denote $[1] = 2$, $[2] = 3$, and $[3] = 1$. The desired distance between agents i and $[i]$ is d_i; here the d_is are positive numbers and satisfy the triangle inequalities: $d_1 + d_2 > d_3\,, d_2 + d_3 > d_1\,, d_1 + d_3 > d_2$.

Cao *et al.* in [26, 27, 28] have studied how to control three autonomous agents to achieve a prescribed triangular formation. If agent i for $i \in \{1, 2, 3\}$ measures the relative position of agent $[i]$ in its own coordinate system, shown in Fig. 1(a), the agents' dynamics can be described by

$$\begin{aligned} \dot{x}_1 &= -k\,(x_1 - x_2)(||x_1 - x_2||^2 - d_1^2)\,, \\ \dot{x}_2 &= -k\,(x_2 - x_3)(||x_2 - x_3||^2 - d_2^2)\,, \\ \dot{x}_3 &= -k\,(x_3 - x_1)(||x_3 - x_1||^2 - d_3^2)\,, \end{aligned} \tag{1}$$

where k is a positive constant to regulate the convergence speed of the formation. For the other case, if agent 2 measures the relative position of agent 1, and agent

3 measures those of agents 1 and 2 in their own coordinates, shown in Fig. 1(b), the agents' dynamics can be written as

$$\begin{aligned}
\dot{x}_1 &= 0\,, \\
\dot{x}_2 &= k\,(x_1 - x_2)(||x_1 - x_2||^2 - d_1^2)\,, \\
\dot{x}_3 &= -k\,(x_3 - x_1)(||x_3 - x_1||^2 - d_3^2) \\
&\quad + k\,(x_2 - x_3)(||x_2 - x_3||^2 - d_2^2)\,.
\end{aligned} \tag{2}$$

In [27, 28], it has been proven that under such gradient-based control laws, system (1) (or (2)) can be stabilized almost globally to an equilibrium corresponding to the triangular formation with the desired shape. Let

$$e_i \triangleq ||x_i - x_{[i]}|| - d_i\,, \tag{3}$$

for $i = 1, 2, 3$. The desired formation set can be described by

$$\mathcal{E} \triangleq \{x :\, e_1 = \, e_2 = \, e_3 = 0\}\,.$$

Let $\mathcal{N}$ be the set of points corresponding to the three agent positions which are collinear in the plane. We summarize their main results as follows:

Theorem 1. *[26, 27, 28] Every trajectory of system (1) (or (2)) starting outside of $\mathcal{N}$, converges exponentially to a finite limit in $\mathcal{E}$.*

In addition, every trajectory of system (1) (or (2)) starting in $\mathcal{N}$ will remain collinear. In practice, collinear positions are easy to become non-collinear because of noise and imprecision in measurements. The equilibra in $\mathcal{N}$ are sensitive to perturbations and thus unstable.

3. Main Results: Multiple Agent Formations

Now we consider the formation task in the plane for $N > 3$ agents. The main idea to accomplish the task is: we choose the three agents of the initial triangular formation to be three leaders for the whole formation and then the other agents join the leaders as followers to realize a large formation. We choose one target configuration that satisfies the prescribed formation shape to be

$$p = [p_1^\top, \ldots, p_N^\top]^\top\,, \tag{4}$$

where $p_i \in \mathbb{R}^2$ represents the position of agent i in some reference coordinate system.

In fact, we adopt two types of controllers for the whole group of agents. First, we control agents $1, 2$ and 3 to meet their distance constraints, which have been introduced in Section 2. Second, we design a new type of controller in (8) for the follower agents, which will be presented in this section.

Before going into the details of the controller design, we introduce some useful graph notations [32]. A node v is *k-reachable* from a set $\mathcal{R}$ of nodes if

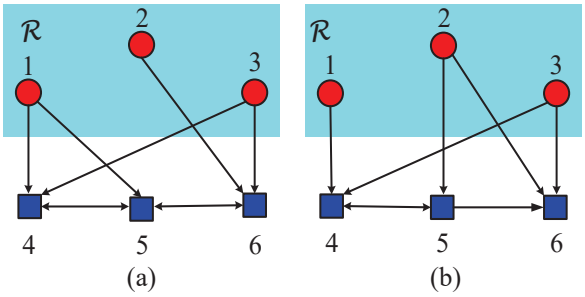

Figure 2: (a) A graph is 3-rooted with roots in set $\mathcal{R}$. (b) A graph is not 3-rooted, since vertex 5 is not 3-reachable from set $\mathcal{R}$.

there are k disjoint paths from k different nodes in $\mathcal{R}$ to node v, where every disjoint path contains only one node in $\mathcal{R}$. A directed graph is *k-rooted*, if there exists a subset of k nodes called roots, from which every other node is k-reachable. We take Fig. 2 as an example. Fig. 2(a) is 3-rooted with roots in set $\mathcal{R}$; Fig. 2(b) is not a 3-rooted graph, since node 5 is not 3-reachable from set $\mathcal{R}$.

We use graph $\mathbb{G}$ to describe the neighbor relationship in the formation. In our problem, graph $\mathbb{G}$ satisfies the following condition.

Assumption 1. *Suppose that graph $\mathbb{G}$ is 3-rooted and vertices $1, 2, 3$ are the three roots of the graph.*

Assumption 1 suggests that nodes $1, 2, 3$ are not affected by any node from the vertex set $\{4, \ldots, N\}$. Fig. 2(a) shows a 3-rooted graph, in which an edge from node i to j represents that j can acquire the relative position of i. Node i is called an in-neighbor of node j.

We treat agents $1, 2, 3$ that form the triangular formation as leaders and the remaining agents in the group as followers. Let $x_l = [x_1^\top, x_2^\top, x_3^\top]^\top$ and $x_f = [x_4^\top, \ldots, x_N^\top]^\top$. Then, the dynamics of the whole N agent system satisfy:

$$\dot{x}_l = F(x_l)\,, \tag{5}$$
$$\dot{x}_f = G(x_f, x_l)\,. \tag{6}$$

The equation (5) describes the dynamics of the three leaders (1) (or (2)). From Theorem 1, the three agents converge to a triangular formation in $\mathcal{E}$. The three leader agents are required to be initially non-collinear, while the follower agents can start at any initial positions. We treat the three leaders as anchors, also as the three roots of graph $\mathbb{G}$.

In the following, we first design controllers and control gains for the follower agents in subsection 3.1, and then analyze global convergence of all the agents as a whole in subsection 3.2.

3.1. Design of Controllers

Let $\mathcal{N}_i$ denote the set of in-neighbors of vertex i. Since graph $\mathbb{G}$ is 3-rooted, each agent $i \in \{4, \ldots, N\}$ has at least three in-neighbors.

Hence, p_i for $i = 4, \ldots, N$ can be located through a linear combination of its in-neighbors' positions as

$$p_i = \sum_{j \in \mathcal{N}_i} a_{ij}\, p_j\,, \tag{7}$$

where $\sum_{j \in \mathcal{N}_i} a_{ij} = 1$ and a_{ij} are real and may be positive or negative. Here, we set $a_{ii} = 0$. We then design the control law in (6) as follows:

$$\dot{x}_i = \sum_{j \in \mathcal{N}_i} a_{ij}\,(x_j - x_i)\,, \tag{8}$$

for $i = 4, \ldots, N$. Note that $x_f = [p_4^\top, \ldots, p_N^\top]^\top$ is an equilibrium point of (8). In the following, we design the control gains a_{ij}s. Agent i computes a_{ij} for $j \in \mathcal{N}_i$ according to

$$\sum_{j \in \mathcal{N}_i} a_{ij}\,(p_j - p_i) = 0\,, \tag{9}$$

for $i = 4, \ldots, N$. Since each agent $i \in \{4, \ldots, N\}$ has at least 3 in-neighbors, then $|\mathcal{N}_i| \geq 3$. For each i, we arbitrarily pick a set of solutions $\{a_{ij}\,,\, j \in \mathcal{N}_i\}$ for (9) that satisfy $\sum_{j \in \mathcal{N}_i} a_{ij} = 1$. In turn, the chosen solution of a_{ij} for $i = 4, \ldots, N$, $j \in \mathcal{N}_i$ guarantees that (8) has an equilibrium point at $x_f = [p_4^\top, \ldots, p_N^\top]^\top$ when $x_1 = p_1, x_2 = p_2, x_3 = p_3$.

Remark 1. *Although we have used a reference coordinate system and assigned a target configuration p, it is emphasized that we only use local information in terms of relative positions of neighbors in control design, see (8). One can see from (9) that, we have used an assigned target configuration to acquire relative target positions $(p_j - p_i)$, in order to determine the weights a_{ij}s for the controller (8).*

Let L be a generalized Laplacian matrix of graph $\mathbb{G}$, satisfying

$$l_{ij} = \begin{cases} -a_{ij} \quad , & for\ j \neq i,\ i = 4, \cdots, N \\ \displaystyle\sum_{j \in \mathcal{N}_i} a_{ij}, & for\ j = i,\ i = 4, \cdots, N, \end{cases} \tag{10}$$

and $l_{ij} = 0$ for $i = 1, 2, 3$ and $j = 1, \cdots, N$. Matrix L can be rewritten as $L = \begin{bmatrix} \mathbf{0} & \mathbf{0} \\ L_{fl} & L_f \end{bmatrix}$ where $L_f \in \mathbb{R}^{(N-3)\times(N-3)}$, $L_{fl} \in \mathbb{R}^{(N-3)\times 3}$, and $\mathbf{0}$s are matrices with all 0s of appropriate dimensions. So, (8) can be written in the compact form

$$\dot{x}_f = -(L_{fl} \otimes I_2)x_l - (L_f \otimes I_2)x_f\,, \tag{11}$$

with $x_l = [p_1^\top, p_2^\top, p_3^\top]^\top$.

Since agents $1, 2, 3$ are not affected by the nodes from the node set $\{4, \ldots, N\}$ and have been proven to converge a triangular formation, it is left to prove the convergence of agents $\{4, \ldots, N\}$. In the following, we introduce a modified matrix of L to stabilize the dynamics of the follower agents.

Lemma 1. *[32] For a generalized Laplacian L of a graph $\mathbb{G}$ with vertex set $\mathcal{V}$, if $\mathbb{G}$ is k-rooted with the root set $\mathcal{R} = \{r_1, \cdots, r_k\}$, then all the principal minors of $L_{\mathcal{V}\setminus\mathcal{R}}$ are distinct from zero, where $L_{\mathcal{V}\setminus\mathcal{R}}$ is the sub-matrix of L with the rows and columns corresponding to nodes in $\mathcal{R}$ crossed out.*

Lemma 2. *[31, 33] Let A be an $n \times n$ real matrix with all of its leading principal minors being nonzero. Then there is an $n \times n$ diagonal matrix D such that all the eigenvalues of DA have positive real parts.*

Remark 2. *The method to construct the matrix D has been provided by Algorithm 3.1 in [31] or by the proof of Theorem 1 in [33]. The construction of D is summarized as follows. Let $A^{(i)}$ be A's leading principal submatrix of order i. For $i = 1, 2, \ldots, n$, repeat the following procedure: find d_i to assign the eigenvalues of $\mathrm{diag}(d_1, \ldots, d_i)\, A^{(i)}$ in the right half plane. Then, it returns $\mathrm{diag}(d_1, \ldots, d_n)$ as one candidate for D.*

Theorem 2. *Suppose that Assumption 1 holds. There exists a diagonal matrix $D = \begin{bmatrix} \mathbf{0}_{3\times 3} & \\ & D_f \end{bmatrix}$ where $D_f \in \mathbb{R}^{(N-3)\times(N-3)}$ is a diagonal matrix, such that the matrix DL, i.e.,*

$$D \begin{bmatrix} \mathbf{0}_{3\times 3} & \mathbf{0} \\ L_{fl} & L_f \end{bmatrix}$$

has three zero eigenvalues and $N-3$ eigenvalues in the right half plane.

Proof: Since $\mathbb{G}$ is 3-rooted, then by Lemma 1, it follows that for the Laplacian matrix $L = \begin{bmatrix} \mathbf{0} & \mathbf{0} \\ L_{fl} & L_f \end{bmatrix}$, all principal minors of L_f are nonzero. Thus, from Lemma 2, there exists a diagonal matrix $D_f = \mathrm{diag}(d_4, \cdots, d_N)$ such that all the eigenvalues of $D_f L_f$ are in the right half plane.
Let $D = \mathrm{diag}(\mathbf{0}, D_f)$ in which $\mathbf{0} \in \mathbb{R}^{3\times 3}$. Then

$$DL = \begin{bmatrix} \mathbf{0} & \mathbf{0} \\ \mathbf{0} & D_f \end{bmatrix} \begin{bmatrix} \mathbf{0} & \mathbf{0} \\ L_{fL} & L_f \end{bmatrix} = \begin{bmatrix} \mathbf{0} & \mathbf{0} \\ D_f L_{fL} & D_f L_f \end{bmatrix}, \tag{12}$$

where matrices $\mathbf{0}$s have appropriate dimensions. So the eigenvalues of DL consist of three zero eigenvalues and the eigenvalues of $D_f L_f$. □

Matrix DL can be used to replace the original L and stabilize the linear system

$$\begin{bmatrix} \dot{x}_l \\ \dot{x}_f \end{bmatrix} = -\left(D \begin{bmatrix} \mathbf{0} & \mathbf{0} \\ L_{fl} & L_f \end{bmatrix} \otimes I_2 \right) \cdot \begin{bmatrix} x_l \\ x_f \end{bmatrix}. \tag{13}$$

We consider DL to be another Laplacian associated with $\mathbb{G}$ because D is a diagonal matrix just scaling each row of L.

System (13) can be rewritten as $\dot{x}_l = \mathbf{0}$ and

$$\dot{x}_f = -(D_f L_{fl} \otimes I_2) x_l - (D_f L_f \otimes I_2) x_f \,. \tag{14}$$

Using Theorem 2, controller (11) is modified to (14). The modification is important to the controller design, which is aimed to stabilize the dynamics of follower agents. The control law (14) can be explicitly written as

$$\dot{x}_i = \sum_{j \in \mathcal{N}_i} d_i \, a_{ij} \, (x_j - x_i) \quad \text{for } i = 4, \ldots, N. \tag{15}$$

Remark 3. *The controller for each follower agent is implemented in its own local coordinate. The properties of 3-rooted graphs guarantee that each follower agent can access the relative positions of its at least three in-neighbors. Thus, using (15), each follower agent converges to its desired position in the plane with respect to its in-neighbors' relative positions in its local coordinate system.*

Remark 4. *The control law (15) is not a consensus-type controller (e.g., the ones in [15, 16, 18, 20, 21, 34, 35]), even though they share similarity in the format. We illustrate the major differences between the classical consensus-type controller and our controller (15) in two aspects: interaction graph and coordinate system. For the consensus-type control law, the interaction graph is required to be connected or to contain a spanning tree, and does not have any requirement for edge weights; all agents are required to share a global coordinate system or at least to share a common sense of direction. For our proposed control law, the interaction graph is required to be 3-rooted, and its weights a_{ij}s have to be assigned according to a prescribed formation shape; there is no need of a common coordinate system or sense of direction, and each agent implements its controller in its own local coordinate. The differences between the consensus-type and the proposed control laws are summarized in Table 1.*

Table 1: Differences between the consensus-type and the proposed control laws.

	Consensus-type control law	Proposed control law
Interaction graph	Connectedness or existence of a spanning tree	3-rooted graph with edge-weights to be assigned
Coordinate system	A global coordinate system or a common sense of direction	Local coordinate systems

Remark 5. *Recent papers [34, 35, 36] study formation control of multi-agent systems with linear dynamics and switching interaction topologies. Paper [35] considers multiple leaders in the formation tracking task. The controllers in these papers are consensus-type, and they require a common direction aligned in local coordinate systems. The major novelty of our work lies in that we solve the formation problem without a common coordinate system. Hence, the methodology adopted in these papers is quite different from ours.*

3.2. Convergence Analysis

In the above subsection, we have designed matrix D and weights for L in controller (14) that are applied to follower agents. In this subsection, we prove the stability of the agents in the formation task.

We first analyze the equilibrium of the whole system. Suppose that $x_l(t)$ converges to certain constant $\bar{p}_l$ at the steady state. From (14), x_f-system has a unique equilibrium point satisfying $(D_f L_f \otimes I_2)x_f = -(D_f L_{fl} \otimes I_2)\bar{p}_l$, since $D_f L_f$ is negative definite. This implies that the final positions of the follower agents depend on the final positions of leader agents. Let $\bar{p}_f$ denote the equilibrium point (i.e., the final position vector) of x_f. Suppose that the positions of all the agents converge to $\bar{p} = [\bar{p}_l^\top, \bar{p}_f^\top]^\top$ in a chosen global reference coordinate system. $\bar{p}$ is unnecessarily equal to p, while our formation task requires that $\bar{p}$ *preserves* the formation shape of p. To facilitate the description of the preservation of formation shape, we introduce a rotation matrix

$$R = \begin{bmatrix} \cos\theta & -\sin\theta \\ \sin\theta & \cos\theta \end{bmatrix},$$

and a translation vector $\tau \in \mathbb{R}^2$. Then, the preservation of formation shape can be understood as follows: there exist a rotation matrix R and a translation vector $\tau \in \mathbb{R}^2$ such that $\bar{p}_i = Rp_i + \tau$ holds for all $i = 1, \ldots, N$. It means that $\bar{p}$ can be obtained from p by a certain coordinate transformation including a rotation and a translation.

The following proposition holds for the pair of final positions $\bar{p}_l, \bar{p}_f$ of the leaders and followers:

Theorem 3. *Let* $\bar{p}_l = [\bar{p}_1^\top, \bar{p}_2^\top, \bar{p}_3^\top]^\top$, $\bar{p}_f = [\bar{p}_4^\top, \ldots, \bar{p}_N^\top]^\top$, *where* $\bar{p}_i = Rp_i + \tau$ *holds for all* $i = 1, \ldots, N$. *It holds that*

$$(D_f L_{fl} \otimes I_2)\,\bar{p}_l + (D_f L_f \otimes I_2)\,\bar{p}_f = \mathbf{0}\,. \tag{16}$$

Proof: Note that $\bar{p}_i = Rp_i + \tau$ holds for all $i = 1, \ldots, N$. Then, one has

$$\begin{aligned} \sum_{j \in \mathcal{N}_i} a_{ij}(\bar{p}_j - \bar{p}_i) &= \sum_{j \in \mathcal{N}_i} a_{ij}(Rp_j + \tau - Rp_i - \tau) \\ &= R \sum_{j \in \mathcal{N}_i} a_{ij}(p_j - p_i)\,. \end{aligned}$$

According to (9), $\sum_{j \in \mathcal{N}_i} a_{ij}(p_j - p_i) = 0$ for $i = 4, \ldots, N$. Hence, one has

$$\sum_{j \in \mathcal{N}_i} a_{ij}(\bar{p}_j - \bar{p}_i) = 0, \quad \text{for } i = 4, \cdots, N. \tag{17}$$

Noticing the definition of L in (10), equation (17) can be rewritten in the compact form:

$$(L_{fl} \otimes I_2)\,\bar{p}_l + (L_f \otimes I_2)\,\bar{p}_f = 0\,.$$

Therefore, (16) is achieved by multiplying D_f on the both sides of the above equation. □

Weights a_{ij}s at the right-hand side of controller (14) are constructed by using a prescribed configuration p. Theorem 3 illustrates that the position pair $[\bar{p}_l^\top, \bar{p}_f^\top]^\top$ of the followers and leaders is an equilibrium of (14). $\bar{p}$ preserves the shape of p.

The design of controller (14) and its control gains as well as Theorems 2 & 3 are necessary preparations for the proof of the whole system's convergence. Then, we study the convergence of all the agents in the theorem below:

Theorem 4. *Under Assumption 1 and matrices D and L designed in the subsection 3.1, the system of $\begin{bmatrix} x_l \\ x_f \end{bmatrix}$ with the dynamics described by (5) and (14), i.e.,*

$$\begin{aligned} \dot{x}_l &= F(x_l) \\ \dot{x}_f &= -(D_f L_{fl} \otimes I_2) x_l - (D_f L_f \otimes I_2) x_f \end{aligned}$$

is asymptotically stable. To be specific, x_l converges to a point in the equilibrium set $\{(x_1, x_2, x_3) : e_1 = e_2 = e_3 = 0\}$ as long as agents $1, 2, 3$ are not initially collinearly positioned; x_f converges to a state which satisfies the formation shape constraints as p_f has.

Proof: We prove the theorem in the following two steps. First, we have shown that $\dot{x}_l = F(x_l)$ is stable. From Theorem 1, the three agents described by (1) (or (2)) globally converge to the equilibrium point set

$$\{x_l : \|x_1 - x_2\| = d_1, \|x_2 - x_3\| = d_2, \|x_3 - x_1\| = d_3\} ,$$

as long as these agents are not initially collinearly positioned. Let the three agents' stable positions to be $x_1 = \bar{p}_1, x_2 = \bar{p}_2, x_3 = \bar{p}_3$. Positions $\bar{p}_1, \bar{p}_2, \bar{p}_3$ and p_1, p_2, p_3 determine a rotation matrix R and a translation vector τ such that $\bar{p}_i = Rp_i + \tau$ holds for $i = 1, 2, 3$.
Second, we prove that x_i globally converges to $Rp_i + \tau$ (i.e., $\bar{p}_i$) for $i = 4, \ldots, N$. From Theorem 3, one can see that $x_f = [\bar{p}_4^\top, \ldots, \bar{p}_N^\top]^\top$ is an equilibrium point of system (14) when $x_l = [\bar{p}_1^\top, \bar{p}_2^\top, \bar{p}_3^\top]^\top$. Next, we prove $x_f = [\bar{p}_4^\top, \ldots, \bar{p}_N^\top]^\top$ is globally stable. To facilitate the analysis, the equilibrium point of the whole system is shifted to the origin by a change of variables. Let $y_l = x_l - \bar{p}_l$ and $y_f = x_f - \bar{p}_f$. From (14), one has

$$\begin{aligned} \dot{y}_f = \dot{x}_f = -(D_f L_{fl} \otimes I_2)\, x_l - (D_f L_f \otimes I_2)\,(x_f - \bar{p}_f) \\ - (D_f L_f \otimes I_2)\, \bar{p}_f \,. \end{aligned} \tag{18}$$

From Theorem 3, $(D_f L_{fl} \otimes I_2)\, \bar{p}_l + (D_f L_f \otimes I_2)\, \bar{p}_f = \mathbf{0}$. Substituting $(D_f L_{fl} \otimes I_2)\, \bar{p}_l$ for $-(D_f L_f \otimes I_2)\, \bar{p}_f$ in (18), one obtains that

$$\dot{y}_f = -(D_f L_{fl} \otimes I_2)\, y_l - (D_f L_f \otimes I_2)\, y_f \,. \tag{19}$$

Construct the Lyapunov function $V(t) = \frac{1}{2} y_f^\top\, y_f$. The derivative of V along the trajectories of system (19) is given by

$$\begin{aligned}\dot{V}(t) =& y_f^\top\, \dot{y}_f \\ =& -\, y_f^\top\, (D_f L_f \otimes I_2)\, y_f - y_f^\top\, (D_f L_{fl} \otimes I_2)\, y_l\,.\end{aligned}$$

Note that y_l converges to $\mathbf{0}$. For $\delta > 0$ and sufficiently large t, y_l is small enough such that if $\|y_f\| \geq \delta$, then $\dot{V} \leq -\frac{1}{2}\, y_f^\top (D_f L_f \otimes I_2)\, y_f$. This implies that $\|y_f\| < \delta$ for large enough t. Therefore, $\lim_{t\to\infty} \|y_f\| = 0$, which means that x_f converges to $\bar{p}_f$. This completes the proof. □

Theorem 5. *The unforced system of (19) (i.e., the system when taking $y_l = \mathbf{0}$) is globally exponentially stable. The convergence speed of $y_f(t)$ is estimated by*

$$\|y_f(t)\| \leq \|y_f(0)\|\, e^{-\lambda_0 t}\,, \tag{20}$$

where

$$\lambda_0 = \min\nolimits_{1\leq i\leq N-3}[\mathrm{Re}(\lambda_i\,(D_f L_f))]\,. \tag{21}$$

Proof: Note that $y_l = x_l - p_l = \mathbf{0}$ when $x_l = [p_1^\top, p_2^\top, p_3^\top]^\top$. Then, (19) can be written as

$$\dot{y}_f = -(D_f L_f \otimes I_2)\, y_f\,. \tag{22}$$

From the proof of Theorem 2, all the eigenvalues of $D_f L_f$ are in the right half plane. Therefore, the y_f-system (19) has a globally exponentially stable equilibrium point at the origin $y_f = \mathbf{0}$ when $y_l = \mathbf{0}$. It means that, the x_f-system (14) has a globally exponentially stable equilibrium point at $x_f = p_f$ when $x_l = p_l$. From (22), the convergence speed of y_f is estimated by $\|y_f(t)\| \leq \|y_f(0)\|\, e^{-\lambda_0\, t}$, where constant λ_0 has been defined in (21). This completes the proof. □

From Theorem 5, one has $\|x_f(t) - \bar{p}_f\| \leq \|x_f(0) - \bar{p}_f\|\, e^{-\lambda_0\, t}$, which implies that $x_f(t)$ exponentially converges to its equilibrium after the stabilization of the three leader agents.

Remark 6. *The application of gradient-based control to the leader agents is necessary. Based on the three leader agents, we are able to design linear controllers incorporating relative positions between the newly-added agents and their neighbors, to globally stabilize the enlarged formation. The control of the leader agents is coordinate-free. Thus, the control of the enlarged formation based on the leader agents is also coordinate-free. A recent paper [37] also studied global stabilization of enlarged formations under agents' local coordinates. However, it uses a different approach – Laman graphs, and explores a class of rigid graphs for which triangulated formations are almost globally stable.*

Remark 7. *Like gradient-based control method, the proposed method is also implemented in agents' local coordinates. Besides, the proposed method shows significant advantages, compared with the gradient-based control method in [5, 8, 22, 23, 24, 25]:* i) *fewer constraints are put on the graph $\mathbb{G}$, i.e., the graph is unnecessary to be rigid;* ii) *the controllers for the follower agents are linear, which is much simpler than the nonlinear gradient-based formation controllers applied in the distance-based control;* iii) *the convergence of the multi-agent system is almost global, while only local convergence is guaranteed. Admittedly, our controller design may increase the cost on solving control gains for a_{ij}s and d_is.*

4. Numerical Simulations

4.1. Example of 6 agents

We give a numerical simulation to validate Theorem 4. We consider 6 agents in the formation task. The graph shown in Fig. 2(a) is a 3-rooted graph with 6 vertices, which describes the desired formation. The prescribed distances between the three leaders (agents) are $d_1 = d_2 = 2\sqrt{2}$ and $d_3 = 4$. Using controller (1) for the three leaders, agents 1, 2 and 3 starting from any non-collinearly initial positions converge to the desired triangular formation. In the simulation, we set k in (1) to be 0.2. According to the desired shape in Fig. 2(a), we assign the target configuration $p = [p_1^\top, \ldots, p_6^\top]^\top = [2, 0, 4, 2, 6, 0, 2, -2, 4, -2, 6, -2]^\top$ for all the agents in some reference coordinate system, shown in Fig. 3. The target configuration is only used to determine a_{ij}s in the following: according to (9) and $\sum_{j\in\mathcal{N}_i} a_{ij} = 1$, one has

$$\begin{aligned} &a_{41}(p_1 - p_4) + a_{43}(p_3 - p_4) + a_{45}(p_5 - p_4) = 0\,,\\ &a_{51}(p_1 - p_5) + a_{54}(p_4 - p_5) + a_{56}(p_6 - p_5) = 0\,,\\ &a_{62}(p_2 - p_6) + a_{63}(p_3 - p_6) + a_{65}(p_5 - p_6) = 0\,, \end{aligned} \tag{23}$$

and

$$\begin{aligned} &a_{41} + a_{43} + a_{45} = 1\,,\\ &a_{51} + a_{54} + a_{56} = 1\,,\\ &a_{62} + a_{63} + a_{65} = 1\,. \end{aligned} \tag{24}$$

By solving the above equations (23) and (24), we obtain a_{ij}s:

$$\begin{bmatrix} a_{41} & a_{43} & a_{45}\\ a_{51} & a_{54} & a_{56}\\ a_{62} & a_{63} & a_{65} \end{bmatrix} = \begin{bmatrix} \frac{1}{2} & -\frac{1}{2} & 1\\ 0 & \frac{1}{2} & \frac{1}{2}\\ -\frac{1}{2} & 1 & \frac{1}{2} \end{bmatrix}.$$

Thus,

$$A = [a_{ij}] = \begin{bmatrix} 0 & 0 & 0 & 0 & 0 & 0\\ 0 & 0 & 0 & 0 & 0 & 0\\ 0 & 0 & 0 & 0 & 0 & 0\\ \frac{1}{2} & 0 & -\frac{1}{2} & 0 & 1 & 0\\ 0 & 0 & 0 & \frac{1}{2} & 0 & \frac{1}{2}\\ 0 & -\frac{1}{2} & 1 & 0 & \frac{1}{2} & 0 \end{bmatrix}.$$

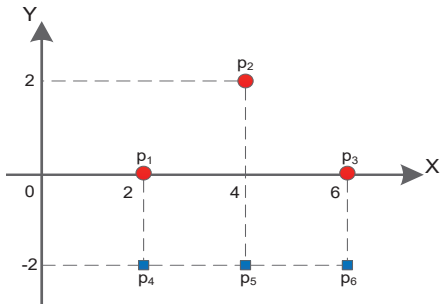

Figure 3: Target configuration p of six agents in some reference coordinate system.

From (10), we obtain the generalized Laplacian L and L_f:

$$L = \left[\begin{array}{c|c} \mathbf{0} & \mathbf{0} \\ \hline L_{fl} & L_f \end{array}\right] = \left[\begin{array}{ccc|ccc} 0 & 0 & 0 & 0 & 0 & 0 \\ 0 & 0 & 0 & 0 & 0 & 0 \\ 0 & 0 & 0 & 0 & 0 & 0 \\ \hline -\frac{1}{2} & 0 & \frac{1}{2} & 1 & -1 & 0 \\ 0 & 0 & 0 & -\frac{1}{2} & 1 & -\frac{1}{2} \\ 0 & \frac{1}{2} & -1 & 0 & -\frac{1}{2} & 1 \end{array}\right],$$

$$L_f = \left[\begin{array}{ccc} 1 & -1 & 0 \\ -\frac{1}{2} & 1 & -\frac{1}{2} \\ 0 & -\frac{1}{2} & 1 \end{array}\right].$$

The eigenvalues of L are $0, 0, 0, 0.134, 1$, and 1.866, which indicate that L has three zero eigenvalues and three positive eigenvalues. Hence, we can set D in Theorem 2 to be the 6-dimensional identity matrix. Applying the controllers in (1) and (14), we run the simulation in Matlab. The initial positions of all the agents are randomly chosen. Fig. 4 shows the evolution of 6-agent formation, in which the final positions of the agents are (-0.59, 9.77), (2.13, 8.98), (1.34, 6.26), (-2.34, 8.80), (-1.38, 7.05), (-0.41, 5.30). From Fig. 4, one can see that all the agents converge to the prescribed formation shape satisfying $\bar{p}_i = Rp_i + \tau$ for all $i = 1, \ldots, 6$, where

$$R = \left[\begin{array}{cc} 0.4825 & 0.8775 \\ -0.8775 & 0.4825 \end{array}\right], \quad \tau = \left[\begin{array}{c} -1.555 \\ 11.525 \end{array}\right].$$

Fig. 5(a) shows the evolutions of the errors e_i defined in (3) for $i = 1, 2, 3$; Fig. 5(b) shows the evolutions of the errors $\|x_i - \text{Fina\_p}_\text{i}\|$ for $i = 4, 5, 6$. From Fig. 5, one can see that agents $1, 2, 3$ are stabilized in a very short time, and that agents $4, 5, 6$ exponentially converge to the prescribed formation after the stabilization of the three leader agents. It validates the conclusions in Theorem 4.

4.2. Example of 9 agents

We give another numerical example to validate Theorem 4. Fig. 6 shows the prescribed formation, in which agents 1,2, and 3 are the three roots of the

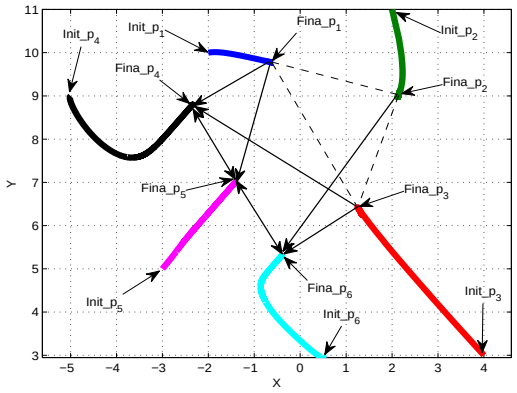

Figure 4: Evolution of 6-agent formation converging to the desired shape shown in Fig. 2(a). The red, green, blue, black, magenta and cyan colors stand for agents 1, 2, 3, 4, 5 and 6, respectively. The Init_p$_i$ and Fina_p$_i$ represent the initial position and final position of agent i, respectively.

graph. The prescribed distances between the three roots are $d_1 = d_2 = 8$ and $d_3 = 8\sqrt{2}$. The constant k in (2) is set to be 0.2. Using controller (2) for the three leaders, agents 1, 2 and 3 starting from any non-collinearly initial positions converge to the desired triangular formation. We assign the target configuration in some reference coordinate system as

$$p = [\,0, 0, 0, -8, 8, 0, 0, -16, 8, \\ -8, 16, 0, 8, -16, 16, -8, 16, -16\,]^\top,$$

corresponding to the prescribed formation shown in Fig. 6. By (9) and $\sum_{j\in\mathcal{N}_i} a_{ij} = 1$, we calculate a_{ij}s and obtain one of several solutions as follows:

$$A = \left[\ a_{ij}\ \right] = \begin{bmatrix} 0 & 0 & 0 & 0 & 0 & 0 & 0 & 0 & 0 \\ 0 & 0 & 0 & 0 & 0 & 0 & 0 & 0 & 0 \\ 0 & 0 & 0 & 0 & 0 & 0 & 0 & 0 & 0 \\ 0 & 1 & 0 & 0 & -1 & 0 & 1 & 0 & 0 \\ \frac{1}{3} & 0 & 0 & 0 & 0 & 0 & \frac{1}{3} & \frac{1}{3} & 0 \\ 0 & 0 & 1 & 0 & -1 & 0 & 0 & 1 & 0 \\ 0 & 0 & 0 & \frac{1}{2} & 0 & 0 & 0 & 0 & \frac{1}{2} \\ 0 & 0 & 0 & 0 & 0 & \frac{1}{2} & 0 & 0 & \frac{1}{2} \\ 0 & 0 & 0 & 0 & -1 & 0 & 1 & 1 & 0 \end{bmatrix}.$$

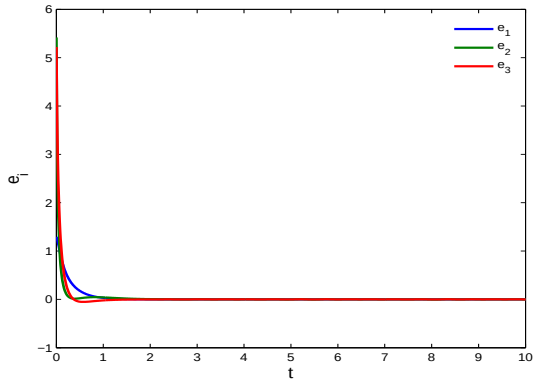

(a)

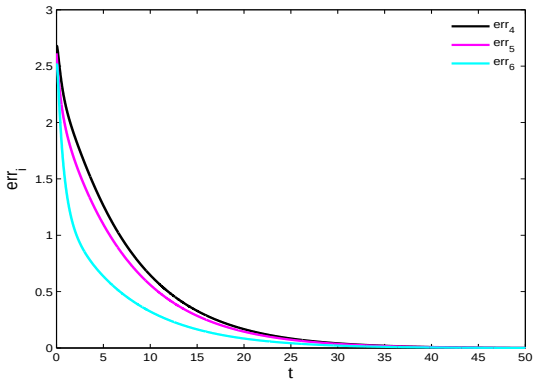

(b)

Figure 5: (a) Evolutions of the errors e_i defined in (3) for $i = 1, 2, 3$; (b) Evolutions of the errors $err_i = \|x_i - \text{Fina\_p}_i\|$ for $i = 4, 5, 6$.

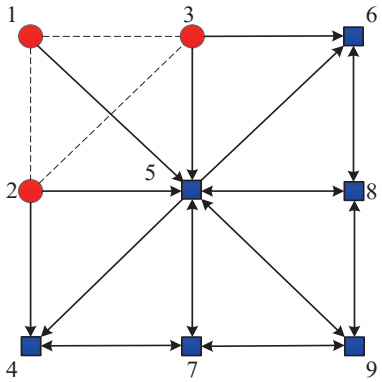

Figure 6: A 3-rooted graph with nine vertices. Vertices 1,2,3 are the three roots of the graph.

From (10), we obtain the generalized Laplacian L:

$$L = \left[\begin{array}{c|c} \mathbf{0} & \mathbf{0} \\ \hline L_{fl} & L_f \end{array}\right]$$

$$= \left[\begin{array}{ccc:ccccccc} 0 & 0 & 0 & 0 & 0 & 0 & 0 & 0 & 0 \\ 0 & 0 & 0 & 0 & 0 & 0 & 0 & 0 & 0 \\ 0 & 0 & 0 & 0 & 0 & 0 & 0 & 0 & 0 \\ \hdashline 0 & -1 & 0 & 1 & 1 & 0 & -1 & 0 & 0 \\ -\frac{1}{3} & 0 & 0 & 0 & 1 & 0 & -\frac{1}{3} & -\frac{1}{3} & 0 \\ 0 & 0 & -1 & 0 & 1 & 1 & 0 & -1 & 0 \\ 0 & 0 & 0 & -\frac{1}{2} & 0 & 0 & 1 & 0 & -\frac{1}{2} \\ 0 & 0 & 0 & 0 & 0 & -\frac{1}{2} & 0 & 1 & -\frac{1}{2} \\ 0 & 0 & 0 & 0 & 1 & 0 & -1 & -1 & 1 \end{array}\right].$$

One can check that L has three zero eigenvalues and six positive eigenvalues. So we take D in Theorem 2 as the 9 by 9 identity matrix. We use the controllers in (13) and run the simulation in Matlab. Fig. 8 shows the evolution of 9-agent formation converging to the prescribed shape in Fig. 6. One can observe in Fig. 8 that the final positions of the agents are $(-6, 4)$, $(-6, -4)$, $(2, 4)$, $(-6, -12)$, $(2, -4)$, $(10, 4)$, $(2, -12)$, $(10, -4)$, $(10, -12)$. Fig. 9(a) shows the evolutions of the errors e_i defined in (3) for $i = 1, 2, 3$; Fig. 9(b) shows the errors $\|x_i - \text{Fina\_p}_\text{i}\|$ for $i = 4, 5, 6, 7, 8, 9$. From Fig. 9, one can see that agents $1, 2, 3$ are stabilized in a very short time, and that agents $4, 5, 6, 7, 8, 9$ exponentially converge to the prescribed formation after the stabilization of the three root agents. It validates the conclusions in Theorem 4.

5. Conclusions

In this work, we have studied formation-keeping tasks in the plane for multiple autonomous agents in their local coordinates. We have treated the three

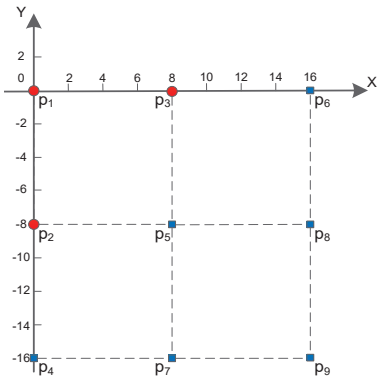

Figure 7: Target configuration p of 9 agents in some reference coordinate system.

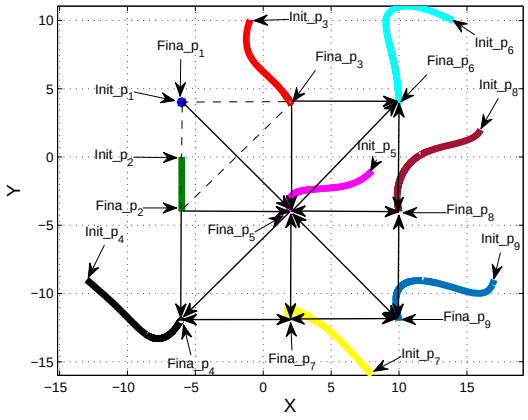

Figure 8: Evolution of 9-agent formation converging to the desired shape shown in Fig. 6. The Init_p and Fina_p represent the initial position and final position, respectively.

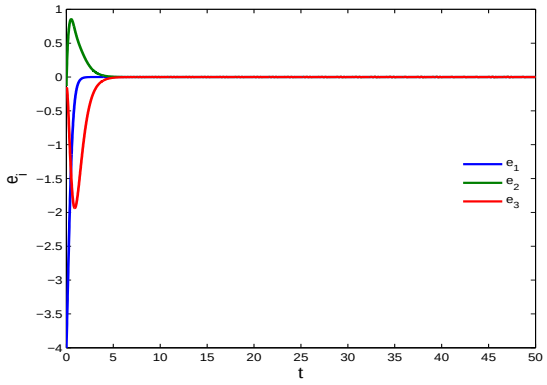

(a)

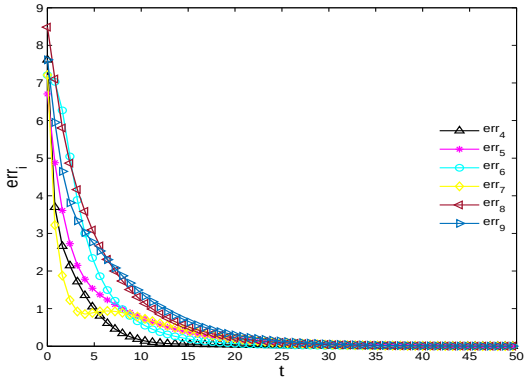

(b)

Figure 9: (a) Evolutions of the errors e_i defined in (3) for $i = 1, 2, 3$; (b) Evolutions of the errors $err_i = \|x_i - \text{Fina\_p}_i\|$ for $i = 4, 5, 6, 7, 8, 9$.

agents in the original triangular formation as leaders and then constructed large formations using properties of rooted graphs. We have proved the stabilization of large formations by designing simple and linear controllers incorporating relative positions between the follower agents and their neighbors. Furthermore, we have proved the global exponential convergence for the stabilization of the follower agents. Since the proposed controllers take simpler forms than most of the existing gradient-based nonlinear controllers, we expect our controllers are easier to be implemented in real robots. So we are currently testing the performance of our controllers using a robotic testbed.

Acknowledgement

The work was supported by the National Natural Science Foundation of China (Nos. 61773175, 61673344, 61403154, 61621003, and 61532020), the National Key Research and Development Program of China (Nos. 2016YFB0800401 and 2017YFC1501301), also by grant from the European Research Council (ERC-StG-2012-307207).

References

[1] F. Bullo, J. Cortes, and S. Martinez. *Distributed Control of Robotic Networks*. Princeton University Press, Princeton, 2009.

[2] J. Fink, A. Ribeiro, and V. Kumar. Robust control of mobility and communications in autonomous robot teams. *IEEE Access*, 1:290–309, 2013.

[3] W. Ren and R. W. Beard. Consensus seeking in multiagent systems under dynamically changing interaction topologies. *IEEE Transactions on Automatic Control*, 50:655–661, 2005.

[4] W. Ren and R. W. Beard. *Distributed consensus in Multi-Vehicle Cooperative Control*. Springer-Verlag New York, Inc., 2008.

[5] B. D. O. Anderson, C. Yu, B. Fidan, and J. Hendrickx. Rigid graph control architectures for autonomous formations. *IEEE Control Systems Magazine*, 28:48–63, 2008.

[6] M. Cao, C. Yu, and B. D. O. Anderson. Formation control using range-only measurements. *Automatica*, 47:776–781, 2011.

[7] B. Grocholsky, E. Stump, P. M. Shiroma, and V. Kumar. Control for localization of targets using range-only sensors. *Experimental Robotics*, 39:191–200, 2008.

[8] L. Krick, M. E. Broucke, and B. A. Francis. Stabilization of infinitesimally rigid formations of multi-robot networks. *International Journal of Control*, 82:423–439, 2009.

[9] E. Stump, V. Kumar, B. Grocholsky, and P. M. Shiroma. Control for localization of targets using range-only sensors. *International Journal of Robotics Research*, 28:743–757, 2009.

[10] M. Turpin, N. Michael, and V. Kumar. Decentralized formation control with variable shapes for aerial robots. In *Proc. of the IEEE International Conference on Robotics and Automation*, pages 23–30, 2012.

[11] P. Ogren, E. Fiorelli, and N. E. Leonard. Cooperative control of mobile sensor networks: Adaptive gradient climbing in a distributed environment. *IEEE Transactions on Automatic Control*, 49(8):1292–1302, 2004.

[12] D. A. M. Stipanović, G. K. Inalhan, R. Teo, and C. J. Tomlin. Decentralized overlapping control of a formation of unmanned aerial vehicles. *Automatica*, 40(8):1285–1296, 2004.

[13] R. W. Beard, J. Lawton, and F. Y. Hadaegh. A coordination architecture for spacecraft formation control. *IEEE Transactions on Control Systems Technology*, 9(6):777–790, 2001.

[14] Kwang-Kyo Oh, Myoung-Chul Park, and Hyo-Sung Ahn. A survey of multi-agent formation control. *Automatica*, 53:424–440, 2015.

[15] W. Ren and E. Atkins. Distributed multi-vehicle coordinated control via local information exchange. *International Journal of Robust and Nonlinear Control*, 17(10-11):1002–1033, 2007.

[16] W. Dong and J. A. Farrell. Cooperative control of multiple nonholonomic mobile agents. *IEEE Transactions on Automatic Control*, 53(6):1434–1448, 2008.

[17] J. A. Fax and R. M. Murray. Information flow and cooperative control of vehicle formations. *IEEE Transactions on Automatic Control*, 49(9):1465–1476, 2004.

[18] R. Olfati-Saber, J. A. Fax, and R. M. Murray. Consensus and cooperation in networked multi-agent systems. *Proceedings of the IEEE*, 95:215–233, 2007.

[19] Z. Lin, B. Francis, and M. Brouche. Local control strategies for groups of mobile autonomous agents. *IEEE Transactions on Automatic Control*, 49:622–629, 2004.

[20] W. Ren, R. W. Beard, and E. Atkins. A survey of consensus problems in multi-agent coordination. In *Proceedings of the American Control Conference*, pages 1859–1864, 2005.

[21] D. V. Dimarogonas and K. J. Kyriakopoulos. A connection between formation infeasibility and velocity alignment in kinematic multi-agent systems. *Automatica*.

[22] J. M. Hendrickx, B. D. O. Anderson, J. C. Delvenne, and V. D. Blondel. Directed graphs for the analysis of rigidity and persistence in autonomous agent systems. *International Journal of Robust and Nonlinear Control*, 17(10-11):960–981, 2007.

[23] S. L. Smith, M. E. Broucke, and B. A. Francis. Stabilizing a multi-agent system to an equilibrium polygon formation. In *Proc. of the 17th MTNS*, pages 2415–2424, 2006.

[24] T. H. Summers, C. Yu, S. Dasgupta, and B. D. O. Anderson. Control of minimally persistent leader-remote-follower and coleader formations in the plane. *IEEE Transactions on Automatic Control*, 56(12):2778–2792, 2011.

[25] C. Yu, B. D. O. Anderson, S. Dasgupta, and B. Fidan. Control of minimally persistent formations in the plane. *SIAM Journal on Control and Optimization*, 48:206–233, 2009.

[26] M. Cao, A. S. Morse, C. Yu, B. D. O. Anderson, and S. Dasgupta. Controlling a triangular formation of mobile autonomous agents. In *Proc. of the 45th IEEE Conference on Decision and Control*, pages 3603–3608, 2007.

[27] M. Cao and A. S. Morse. Maintaining a directed, triangular formation of mobile autonomous agents. *Communications in Information and Systems*, 11:1–16, 2011.

[28] M. Cao, B. D. O. Anderson, A. S. Morse, and C. Yu. Control of acyclic formations of mobile autonomous agents. In *Proc. of the 47th IEEE Conference on Decision and Control*, pages 1187–1192, 2008.

[29] S. Mou, M. Cao, and A. S. Morse. A distributed control law for acyclic formations. In *Proc. of the 18th IFAC world congress*, pages 7818–7823, 2011.

[30] B. D. O. Anderson, C. Yu, S. Dasgupta, and A. S. Morse. Control of a three coleader formation in the plane. *Systems & Control Letters*, 56(9):573–578, 2007.

[31] Z. Lin, W. Ding, G. Yan, C. Yu, and A. Giua. Leader-follower formation via complex laplacian. *Automatica*, 49(6):1900–1906, 2013.

[32] Z. Lin, L. Wang, Z. Chen, M. Fu, and Z. Han. Necessary and sufficient graphical conditions for affine formation control. *IEEE Transactions on Automatic Control*, 61(10):2877–2891, 2016.

[33] C. S. Ballantine. Stabilization by a diagonal matrix. *Proceedings of the American Mathematical Society*, 25(4):728–734, 1970.

[34] X. Dong and G. Hu. Time-varying formation control for general linear multi-agent systems with switching directed topologies. *Automatica*, 73:47–55, 2016.

[35] X. Dong and G. Hu. Time-varying formation tracking for linear multi-agent systems with multiple leaders. *IEEE Transactions on Automatic Control*, 62(7):3658–3664, 2017.

[36] X. Dong, Y. Zhou, Z. Ren, and Y. Zhong. Time-varying formation control for unmanned aerial vehicles with switching interaction topologies. *Control Engineering Practice*, 46:26–36, 2016.

[37] X. Chen, M. A. Belabbas, and T. Başar. Global stabilization of triangulated formations. *SIAM Journal on Control and Optimization*, 55(1):172–199, 2017.